Received: 25 March 2025 | Revised: 17 April 2025 | Accepted: 22 April 2025

DOI: 10.1002/pc.30004

RESEARCH ARTICLE

Polymer COMPOSITES WILEY

Investigation and assessment of mechanical properties of co-extrusion with towpreg continuous carbon fiber reinforced thermoplastic composites manufactured using material extrusion

Nabeel Maqsood[1,2] | **Genrik Mordas**[1] | **Marius Rimašauskas**[3] | **Kateřina Skotnicová**[2] | **Jawad Ullah**[4] | **Joamin Gonzalez-Gutierrez**[5]

[1]3D Technologies and Robotics Laboratory, Department of Laser Technologies, Center for Physical Sciences and Technology, Vilnius, Lithuania

[2]Faculty of Materials Science and Technology, VSB – Technical University of Ostrava, Ostrava, Czech Republic

[3]Department of Production Engineering, Faculty of Mechanical Engineering and Design, Kaunas University of Technology, Kaunas, Lithuania

[4]School of Engineering, Ulster University, Belfast, Northern Ireland, UK

[5]Functional Polymers Research Unit, Materials Research and Technology (MRT) Department, Luxembourg Institute of Science and Technology (LIST), Luxembourg

Correspondence
Nabeel Maqsood, 3D Technologies and Robotics Laboratory, Department of Laser Technologies, Center for Physical Sciences and Technology, Savanoriu Ave. 231, LT-02300, Vilnius, Lithuania.
Email: nabeel.maqsood@ftmc.lt

Funding information
European Commission

Abstract

Additive manufacturing (AM) is an advanced technique to fabricate a complex geometrical structure using polymer, metals, ceramics, and composite materials. Fused filament fabrication (FFF) is the most widely used extrusion-based AM technique to manufacture polymer and composite parts. Continuous carbon fiber (CCF) is a lightweight high-strength material that offers exceptional mechanical durability and performance when incorporated with polymers; it significantly enhances their performance. To print continuous fibers using the material extrusion technique, various methods have been adapted according to the AM technology. In this study, a self-developed co-extrusion with towpreg method was employed to fabricate the continuous fiber polymer composites in which both the materials polymer filament matrix and CCF reinforcement were inserted separately and extruded together through a single nozzle. Two important printing process parameters (layer height and line width) were considered with different ranges to investigate their influence on the mechanical properties (tensile, flexural, shear and compressive), air void volume, and fiber volume fraction. The results obtained demonstrate that both parameters have a significant impact on the properties and are mostly influenced by the layer height of the samples. The group of composite specimens with the layer height of 0.4 mm and line width of 1.0 mm showed the highest tensile, flexural, shear, and compressive strength of 372.68, 247.59, 42.83, and 184.19 MPa, respectively, with the minimum air void volume of 13.84%. Furthermore, the research outcomes highlight that the composites properties can be optimized by adjusting printing process parameters.

Highlights

- Co-extrusion with towpreg process was employed to fabricate CCFRTC.
- Layer height and line width were investigated for their influence on properties.

- The theoretical model was used to predict modulus to validate the model's accuracy.
- The results demonstrated that both the parameters have a significant impact.
- This investigation led to improving the performance of CCFRTCs

KEYWORDS

air void volume, continuous carbon fiber reinforced thermoplastic composites, fused filament fabrication, mechanical properties, printing process parameters

1 | INTRODUCTION

Additive manufacturing (AM), also known as 3D printing, is an emerging fabrication technique that builds components layer by layer from a digital model. It enables the creation of complex geometries using a variety of materials, including polymers, metals, ceramics, and composites.[1–5] Among these, polymer-based AM, especially via fused filament fabrication (FFF) is the most widely adopted due to its simplicity, cost-efficiency, and material versatility.[6–8] However, printed polymer parts often suffer from limited mechanical performance, restricting their use in structural or load-bearing applications.

To address this limitation, reinforcing thermoplastics with fibers either discontinuous (short) or continuous has become a popular approach.[9–11] While short fibers can enhance stiffness and toughness, continuous fibers provide a far superior improvement in mechanical strength, load transfer efficiency, and dimensional stability.[12–15] In particular, continuous carbon fiber (CCF) stands out for its exceptional strength-to-weight ratio, making it highly attractive for aerospace, automotive, and high-performance engineering applications.

Fused filament fabrication (FFF) is the most widely used material extrusion process for manufacturing thermoplastic composites incorporating continuous fiber reinforcements. Several methods have been developed to integrate continuous fibers into the material extrusion process alongside thermoplastic extrusion.[16–18] These methods include filament extrusion, towpreg extrusion, co-extrusion with towpreg, in-situ impregnation, in-situ consolidation, and inline impregnation.[19] F. Wang et al.[20] conducted a comparison study between the towpreg extrusion and in-situ impregnation processes and found that the towpreg extrusion technique increased fiber content by about 7% and reduced void rate by about 6%, resulting in 19% and 20% increases in tensile and flexural strengths for the 3D-printed polymer composite structures, respectively. However, their study was limited to 1 K fiber systems, whereas our work focuses on 3 K fibers and dual-parameter optimization using a co-extrusion head. Typically, FFF 3D printers are modified with extrusion heads that feature dual input channels one— for continuous fibers and one for thermoplastic filament converging— into a single output extrusion nozzle.[21–23] This design enables the fabrication of 3D-printed thermoplastic composites.

Among continuous fiber composites, continuous carbon fiber (CCF) reinforced composites are particularly noteworthy for their exceptional properties, offering lightweight, durable structures with high stiffness and strength. CCF-reinforced thermoplastic composites (CCFRTC) have demonstrated significant mechanical strength, making them ideal for lightweight structures. However, producing such composites via 3D printing poses several challenges, including achieving high-quality surface finishes, which are crucial for optimal mechanical properties.[24,25] The proper control and optimization of the printing process parameters play a critical role in determining the quality of the final product, influencing factors such as fiber volume fraction, air void content, and overall mechanical performance of the composites.[26–31] Therefore, optimization of these parameters is essential to maximize the benefits of CCFRTCs in practical applications. Previous investigators have reported the effect of various printing process parameters (extrusion temperature, extrusion width and extrusion multiplier) keeping the layer thickness constant.[27] However, the effects of the layer height and line extrusion width with the customized printing head for 3 K CCF have not been investigated. Therefore, this investigation was performed.

Recent studies have examined the effects of some of these parameters, but often only one variable is adjusted at a time, or the analysis is limited to specific fiber types such as 1 K carbon tows. For example, Rimašauskas et al.[22] conducted a study on the quality of 3D-printed composite structures, focusing on the effects of printing parameters, specifically layer height and line width, for 1 K impregnated CCF composites to reduce void volume in the polymer structures. Their experimental findings indicated that composite specimens printed with a layer thickness of 0.3 mm and a line width of 1 mm exhibited the lowest volume of air voids, achieving a maximum tensile strength of 183 MPa. Additionally, they observed that reducing the layer thickness and line width improved tensile strength, and increasing the carbon

fiber content led to enhanced mechanical performance.[32] Similarly, Moradi et al.[33] investigated the influence of various printing parameters, such as layer thickness, infill percentage, and extruder temperature, on the maximum failure load of bronze PLA composites. The results demonstrated that a higher layer thickness improved the composite's failure load. Other studies examined the impact of printing parameters including layer resolution, printing orientation, infill density, nozzle diameter, nozzle temperature, and raster angle on the electrical conductivity and mechanical properties of PLA-based short carbon and ABS composites.[34–36] Chen et al.[37] evaluated the optimal printing parameters, such as nozzle diameter, layer thickness, printing speed, and temperature, for 3D-printed continuous glass fiber-reinforced PLA composites. Their study reported a maximum tensile strength of 241 MPa with a 45 wt.% reinforcement content. Additional research focused on the effects of printing speed and layer thickness on the quality of 3D-printed cement-based composite materials.[38] Dou et al.[32] conducted experiments on the tensile properties of 3D-printed 1 K CCF-reinforced PLA composites, considering parameters such as layer height, extrusion width, printing temperature, and speed. Their results showed that decreasing the layer height, extrusion width, and printing speed while increasing the printing temperature led to better mechanical properties. The optimum parameters resulted in a maximum tensile strength of 226.60 MPa and a tensile stiffness of 22.38 GPa. The authors have used various adaptation methods to utilize continuous fiber into FFF technology to manufacture polymer composites and study their mechanical performance.

While several studies have explored the influence of extrusion temperature, infill density, and printing speed on the mechanical properties of 3D printed fiber composites, the combined effect of layer height and line width, particularly using a co-extrusion with towpreg method for 3 K CCF, has not been thoroughly investigated. Previous work on 1 K fiber composites demonstrated improvements in void reduction and mechanical strength with optimal parameters; however, scaling up to 3 K CCF poses unique challenges in fiber placement, bonding, and void control. Thus, there remains a critical need to systematically evaluate how layer height and line width influence key properties such as tensile, flexural, shear, and compressive strengths, fiber volume fraction, and air void content when employing a co-extrusion towpreg strategy. To bridge this gap, this study presents a systematic investigation into the mechanical behavior of continuous 3 K CCF-reinforced thermoplastics fabricated using a self-developed co-extrusion with towpreg method. The influence of two critical process parameters, layer height and line width, is evaluated across six composite groups. The mechanical performance (tensile, flexural, shear, and compressive strength), fiber volume fraction, and void content are quantified. Additionally, theoretical predictions using the rule of mixtures are compared with experimental data to validate model accuracy. This work not only provides insights into process–property relationships but also offers optimization guidelines for high-strength continuous fiber composites using extrusion-based AM.

The novelty of this study lies in the systematic investigation of layer height and line width combinations for 3 K towpreg-based continuous carbon fiber composites using a custom co-extrusion head printing in FFF. While earlier studies have focused primarily on 1 K CCF or fixed layer heights, our work presents a more comprehensive mechanical characterization (tensile, flexural, shear, and compressive) alongside void and fiber volume analysis for a higher strength 3 K fiber system. Furthermore, the integration of a theoretical model (ROM) to predict elastic behavior validated against experimental results adds an analytical layer often absent in prior studies. This combined experimental–theoretical approach offers new insights into process–property relationships and establishes parameter guidelines for optimizing CCFRTC fabrication in future industrial and aerospace applications.

In this study, in situ co-extrusion with the towpreg process was employed to fabricate CCFRTC using the FFF technique. In this process, the impregnated CCF and the thermoplastic matrix material were fed separately into the FFF system, where they fused together, creating a strong bond and extruding the composite material. Six different groups of composites were printed, each varying in layer height and line/ extrusion width, to investigate their influence on the mechanical properties. The mechanical properties were assessed, including tensile, flexural, shear, and compressive strengths. Additionally, the carbon fiber content and air void volume were measured to understand their impact on the composite's performance. A theoretical model was also employed to predict the elastic modulus, and these predictions were compared with the experimental results to validate the model's accuracy. This comprehensive analysis provided insights into how variations in printing parameters affect the structural integrity and mechanical properties of CCFRTCs, guiding future optimizations for enhancing the performance of 3D-printed thermoplastic composites.

2 | MATERIALS AND METHODS

2.1 | Materials used in the experiment

In this research, a polylactic acid (PLA) thermoplastic filament with a diameter of 1.75 mm, sourced from

PolyLite by Polymaker, was employed as the matrix material. The chosen PLA filament has a tensile strength of 46.6 MPa, an elastic modulus of 2.6 GPa, and a density of 1.24 g/cm^3. For reinforcement, a standard 3 K continuous carbon fiber (CCF) tow, specifically the T300B-3000 from Toray, was used. This CCF tow consists of 3000 individual carbon filaments, each with a diameter of 7 μm, and is manufactured from polyacrylonitrile. As per the manufacturer's specifications, the T300B-3000 CCF tow demonstrates a tensile strength of 3530 MPa, a Young's modulus of 230 GPa, and a density of 1.76 g/cm^3.

2.2 | Fabrication of CCFRTC using FFF

Prior to the fabrication process, the CCF was impregnated by dissolving PLA pellets in dichloromethane to prepare towpregs with enhanced printability and adhesion as explained by Rimašauskas et al.[39] The co-extrusion with towpreg method was employed to print the composites, wherein the CCF towpreg was combined with the matrix material (Figure 1A). The composite feedstock was then introduced into the extrusion nozzle, enabling the simultaneous deposition of CCF and the PLA matrix material.[40–42]

For the fabrication of composite specimens, a modified version of the MeCreator 2 (HK GETECH CO., LIMITED, Hong Kong, China) 3D printer was used (Figure 1B). The printer's extrusion head was modified to include two input channels: one for the PLA thermoplastic filament and another for the impregnated CCF (Figure 1C).[21,22] To ensure high-quality fabrication of the CCFRTC structures, a controlled air flow cooling system with a pressure regulator was incorporated to ensure the high quality and fine fabrication of composite structures that is used to cool the deposited material and help to retain the shape of the deposited strands and prevent the flow of the molten polymer.[27] The flow rate of the compressed air cooling was controlled through the digital pressure regulator valve. In the experimental research, 0° unidirectional composite specimens were printed using a rectilinear 100% infill pattern. The printing process parameters for the fabrication of the composite specimen groups are detailed in Table 1.

Figure 1D Illustrates the printed composites produced using the co-extrusion with towpreg method and the modified FFF 3D printer. Table 2 presents the parameters for the group samples prepared for the current experiment. This approach facilitated the creation of composite structures with enhanced mechanical properties, providing valuable insights into the optimization of printing parameters for advanced composite fabrication. The flowchart of the experimental work performed in this research is presented in Figure 2.

TABLE 1 Printing process parameters used to fabricate 3D-printed composite specimens.

Printing settings	Value, description
Extruder temperature	230°C
Extrusion multiplier	0.7
Printing speed	5 mm/s
Air flow cooling	40 L/min
Infill percentage	100%
Printing bed temperature	90°C
Infill density	100%
Infill pattern	Rectilinear
Nozzle diameter	1.5 mm

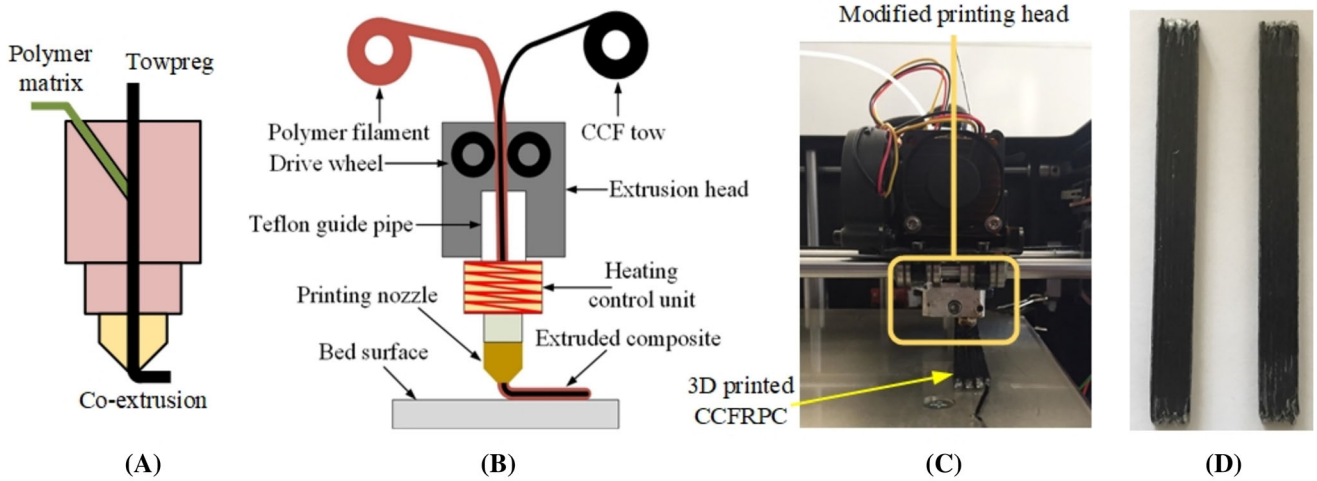

FIGURE 1 Schematic of (A) co-extrusion with towpreg process, (B) FFF process of fabricating CCFRPC using towpreg, (C) modified printing head and 3D printer used for printing the composites for the experiments, and (D) manufactured composites with CCF using FFF.

TABLE 2 Parameters of the group samples based on variation in layer height and line width.

Groups of samples	Group 1	Group 2	Group 3	Group 4	Group 5	Group 6
Layer height (mm)	0.4	0.5	0.4	0.5	0.4	0.5
Line width (mm)	1	1	1.2	1.2	1.4	1.4

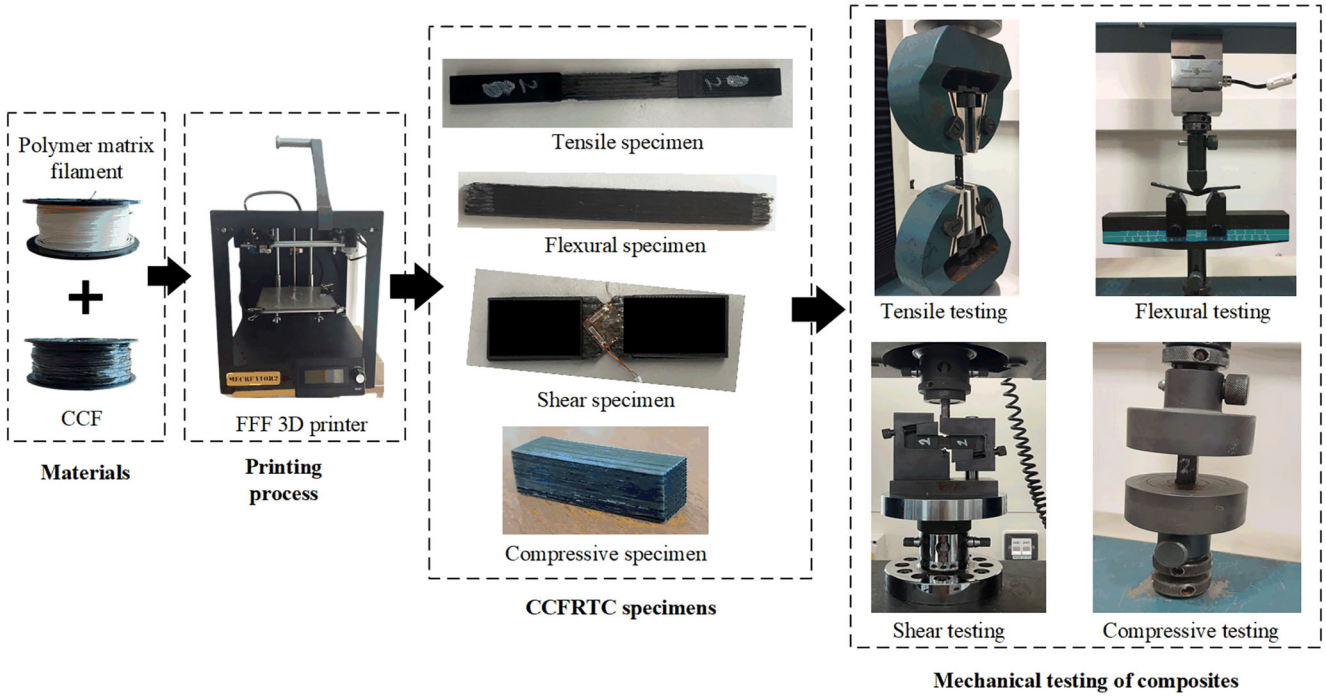

FIGURE 2 Flowchart of the experimental work.

2.3 | Mechanical testing measurement procedure

In the present study, ASTM D3039, ASTM D790, ASTM D5379, and ASTM D695 standards were used to perform the tensile, flexural, shear, and compressive tests, respectively. All the tests were performed using a universal testing machine of Tinius Olsen H25KT having a capacity of 25 kN at room temperature.

For the tensile test, rectangular cross-section solid composite specimens with the dimensions of 150 × 13 × 3 mm were fabricated. Tabs on both ends of the specimen were also 3D-printed separately using PLA material having dimensions of 50 × 12.5 × 2 mm and a bevel angle of 30°. Four strain points were marked on the printed specimen 15 mm apart from the center to measure the elastic strain using optical extensometers. For the tensile test, a 2 mm/min rate of head displacement was used.

For the flexural test, according to standard rectangular cross-section specimens having dimensions of 127 × 12.7 × 3.2 mm were printed. The 3-point bending test was performed using the crosshead motion rate of 1.35 mm/min and span support length of 51.2 mm. According to the above-mentioned testing standards, five specimens for each group were printed to determine their average properties.

For the shear test, a rectangular cross-section composite specimen with the dimensions of 76 × 20 × 2.5 mm was 3D printed. PLA-printed tabs were applied using super glue at each end of the testing specimen having dimensions of 32 × 20 × 1.5 mm for the grip during the testing. Two v-notches were made at the center of the specimen with a 90° angle on both sides separated by 12 mm from the tip of both notches. Strain gauges were applied to the specimen to record the strain displacement caused during the test. A standard head displacement rate of 2 mm/min was used to test the composite parts. Five specimens for each group were printed and tested to determine their average values.

For the compressive test, a rectangular block of composite specimen was manufactured with the dimensions of 12.7 × 12.7 × 25.4 mm. The CCFRTC specimens were printed longer in length and cut to the specific length as

recommended by the standard. The test was performed at a compression rate of 1.3 mm/min. The compressive force was applied in the direction of the printed composite layers, and for each group, five specimens were manufactured for the test.

2.4 | Microstructural fracture interface analysis study

The interfacial adhesion between the matrix and the reinforcement is a critical factor in determining the mechanical performance and structural integrity of composite materials. To evaluate the quality of adhesion and fracture behavior, fractographic analysis was conducted following mechanical testing. This analysis aimed to investigate the fracture interface between the thermoplastic matrix and CCF reinforcement, focusing on the separation mechanisms under tensile loading and identifying the bonding characteristics at failure points. To achieve high-resolution imaging of the fracture surface, a Field Emission Scanning Electron Microscope (FE-SEM) SU5000 (Hitachi Co., Tokyo, Japan) was employed. The obtained micrographs provided detailed insights into the fiber-matrix interfacial adhesion, failure mechanisms, and potential weak zones, allowing a comprehensive assessment of the composite's structural behavior under applied loads.

2.5 | Volume fraction of the fiber

The approximate estimation of CCF content in the composite was calculated using the length of the tool path of the manufactured specimen by knowing the number of lines and layers in width and thickness. Thus, the reinforcement content measured was considered as the weight ratio of carbon fiber to composite specimen,[41] which was converted to the fiber volume fraction V_f (%).

2.6 | Air void content estimation in the composites

The air void volume present in the manufactured polymer composite specimen with varying parameters was theoretically calculated using the following expression.[43]

$$V_v = 100 - (V_r + V_m) \quad (1)$$

where V_v is void volume, V_r is volume percentage of reinforcement content, and V_m is volume percentage of matrix content.

3 | RESULTS AND DISCUSSIONS

3.1 | Tensile properties

The tensile behavior of CCFRTC specimens fabricated with varying layer heights and line widths demonstrated the significant influence of these parameters on their mechanical properties. Stress–strain curves for the six different 3D-printed groups are presented in Figure 3A, illustrating distinct performance variations. Group 1, with a layer height of 0.4 mm and a line width of 1.0 mm, exhibited the highest tensile stress, followed sequentially by Groups 3, 2, 5, and 4. Group 6 recorded the lowest tensile stress, highlighting the critical role of layer height and line width in determining tensile performance.

The tensile properties of the composites, detailed in Figure 3B,C, show a clear trend where decreasing layer height and line width significantly enhance both tensile strength and Young's modulus. Group 1 achieved the highest tensile strength of 372.68 MPa, while the lowest tensile strength, 231.04 MPa, was observed in Group 6, manufactured with a layer height of 0.5 mm and a line width of 1.4 mm. This difference is attributed to the increased fiber volume fraction and reduced air void content in Group 1, enabled by a lower layer height and narrower line width. A smaller layer height results in more layers for a given specimen thickness, improving interlayer adhesion and allowing better resin infiltration around the fibers, which in turn enhances load transfer during tensile loading. Additionally, reduced voids lead to fewer stress concentration points, lowering the likelihood of premature failure.

Similarly, Young's modulus followed the same trend, with Group 1 exhibiting the highest modulus of 41.63 GPa, indicating a stiffer composite. Conversely, Group 6 showed the lowest modulus of 26.17 GPa, correlating with a more flexible behavior. Higher elastic modulus values reflect improved stiffness and rigidity, which are critical for applications requiring high resistance to deformation under tensile loads.

During the tensile testing, strain was recorded using optical extensometers across a 60 mm gauge length. The strain to failure is an important indicator of ductility and energy absorption. For transparency, the average strain to failure of the best-performing group (Group 1) was 1.02% ± 0.07%, and the values for the other groups ranged from 0.56% to 0.98%. These values show that as layer height and line width increase, the composites become more brittle, correlating well with the drop in tensile strength and stiffness. Table 3 represents the values of strain to failure of each composite group.

When comparing the effects of layer height and line width on tensile properties, it is evident that layer height

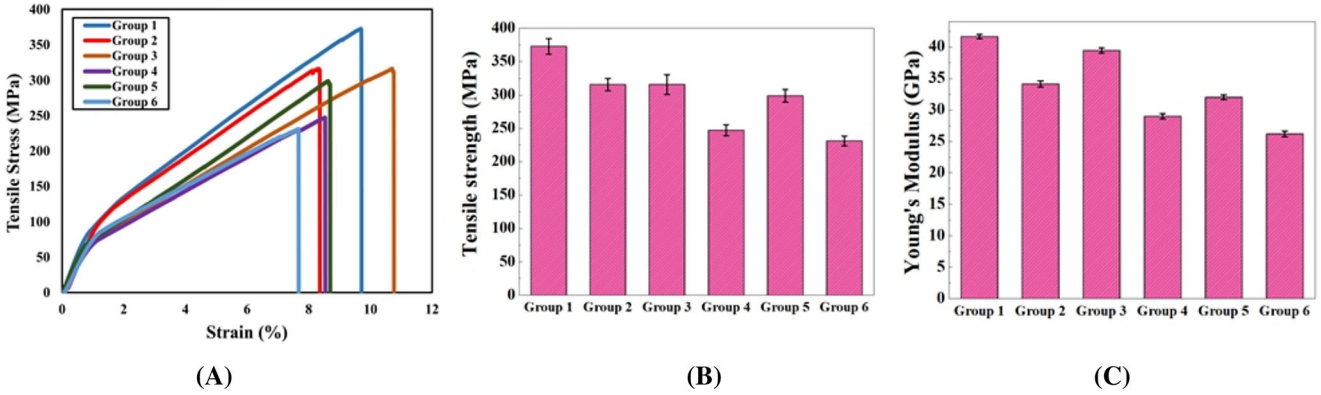

FIGURE 3 Tensile properties of the manufactured CCFRTCs using FFF: (A) representative tensile stress–strain curves of all six specimen groups; (B) average tensile strength with standard deviation; (C) Young's modulus comparison across groups.

TABLE 3 Strain to failure (%) of composite specimens.

Composite groups	Strain to failure (%) ± SD
Group 1	1.02 ± 0.07
Group 2	0.89 ± 0.05
Group 3	0.94 ± 0.06
Group 4	0.67 ± 0.04
Group 5	0.75 ± 0.05
Group 6	0.56 ± 0.03

has a more pronounced influence.[22] While decreasing line width impacts strength to a lesser extent, the results show that even with a layer height of 0.5 mm and a line width of 1.2 mm, the tensile strength was 20.9% lower than Group 5, which had a smaller layer height of 0.4 mm but a wider line width of 1.4 mm. These findings underscore the critical role of layer height in determining the tensile strength of 3D-printed composite structures. Notably, Group 1, with a layer height of 0.4 mm and a line width of 1.0 mm, exhibited a 61.3% higher tensile strength compared to Group 6, highlighting the significant influence of processing parameters on mechanical performance. This substantial difference emphasizes the importance of optimizing layer height to achieve superior tensile properties in continuous fiber-reinforced composites.

However, during tensile testing, a notable proportion of samples fractured near the clamp's tab, a common issue in testing composite materials with rectangular cross-sections.[22,44] This failure mode often arises due to stress concentrations at the clamping area, which can prematurely induce cracking or fracture, thereby affecting the reliability of the measured tensile properties. Addressing such issues through improved specimen preparation and testing methodologies could further enhance the accuracy and reproducibility of tensile property evaluations in 3D-printed composite materials.

The tensile strength of the composite specimen exhibited significant improvements with adjustments to layer thickness and line width during fabrication. Reducing the layer thickness from 0.5 to 0.4 mm while maintaining a line width of 1.0 mm resulted in an 18% increase in tensile strength. Similarly, when the line width was held at 1.2 mm, decreasing the layer thickness to 0.4 mm led to a 27.7% increase in tensile strength. Additionally, reducing the line width from 1.2 to 1.0 mm at a constant layer thickness of 0.4 mm resulted in a further 17.9% improvement in tensile strength. Compared to the work of Heidari-Rarani et al.[23] and Li et al.,[10] who primarily investigated short or chopped carbon fibers, our results demonstrate that using continuous 3 K CCF in a co-extrusion system yields superior strength and stiffness, even with limited parameter variation. This highlights the importance of fiber continuity and optimized deposition conditions.

These trends can be attributed to the interplay between layer thickness and line width, where decreasing the layer thickness increases the total number of layers in the structure. This modification not only enhances the composite's density but also increases the carbon fiber volume fraction (as discussed in Section 3.5), both of which significantly contribute to the tensile strength of the composite.[22] The increased number of layers promotes better interlayer adhesion and load transfer, while higher fiber content amplifies the load-bearing capacity, culminating in improved mechanical performance. These findings underscore the importance of optimizing printing parameters to enhance the structural and mechanical properties of 3D-printed continuous fiber-reinforced composites.

3.2 | Flexural properties

The flexural properties of the CCFRTC specimens were evaluated through three-point bending tests, revealing

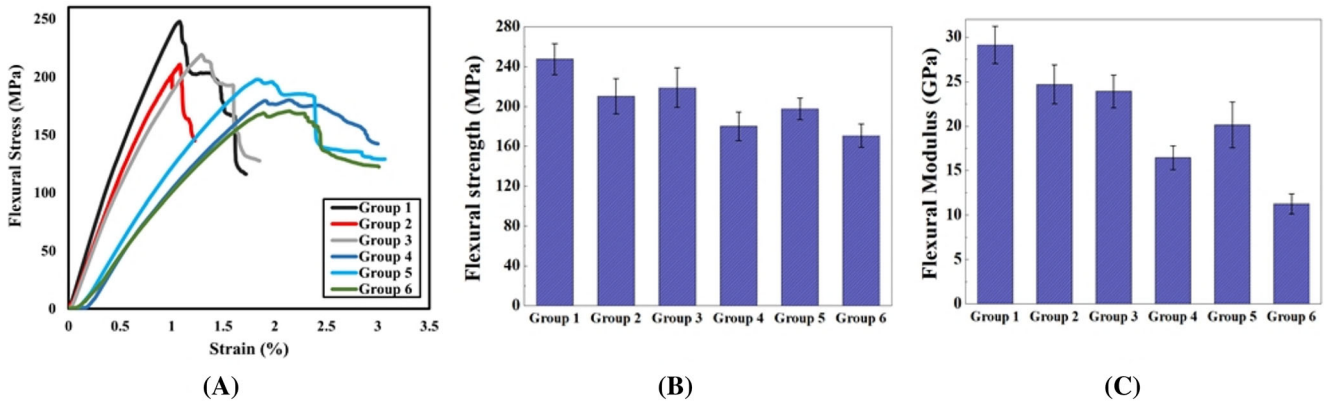

FIGURE 4 Flexural properties of 3D-printed CCFRTCs using FFF: (A) Flexural stress–strain curves from three-point bending tests; (B) average flexural strength with standard deviation; (C) Flexural modulus.

distinct performance differences among composite groups fabricated with varying layer heights and line widths. The flexural stress–strain curves, illustrated in Figure 4A, demonstrate trends consistent with those observed in the tensile stress–strain curves. Group 1, manufactured with a 0.4 mm layer height, exhibited the highest flexural stress, followed sequentially by Groups 3, 2, 5, 4, and finally Group 6, which displayed the lowest flexural stress. The higher flexural strength of Group 1 can be attributed to its reduced layer height and line width, which minimized void formation within the composite structure. Lower void content enhances interlaminar bonding and adhesion between layers, enabling more efficient stress transfer under flexural loading. In contrast, increasing layer height and extrusion width in other groups led to higher void content and weaker interlaminar adhesion, resulting in reduced flexural strength.

The flexural strength and modulus of the CCFRTC specimens are presented in Figure 4B,C, respectively, highlighting the significant impact of layer height and line width on the flexural properties. The results reveal that reducing both parameters maximizes the flexural strength and modulus, with Group 1 achieving the highest values of 247.59 MPa and 29.13 GPa, respectively. The average flexural strength for Groups 2, 3, 4, and 5 was 210.48, 218.99, 180.23, and 197.81 MPa, respectively, while Group 6 exhibited the lowest flexural strength and modulus, measured at 170.70 MPa and 11.26 GPa. These findings demonstrate that layer height plays a more dominant role in influencing flexural performance, consistent with the trends observed in the tensile property analysis. In flexural testing, stresses are concentrated at the outermost fibers. Lower layer height increases the number of these fibers in load-bearing zones and improves bonding between layers, allowing more effective resistance to bending moments. This justifies the higher modulus and strength observed in Group 1.

While reducing extrusion width alone has a limited impact on flexural properties, its effect becomes more pronounced when paired with a lower layer height.[21,45] This combination facilitates the formation of a denser structure with improved interlayer bonding and reduced void content, contributing to enhanced mechanical performance (see Section 3.6).

3.3 | Shear properties

The shear stress–strain curves of the six composite groups, fabricated with varying layer heights and line widths, are presented in Figure 5A. These curves highlight the inverse performance of the specimens under shear loading, demonstrating the significant impact of these parameters on the shear properties of the composites.

Similar to the trends observed in tensile and flexural loading, Group 1 exhibited the highest peak shear stress, followed sequentially by Groups 3, 2, 5, and 4, with Group 6 showing the lowest shear stress. The superior performance of Group 1 can be attributed to its reduced layer height and line width, which facilitate the formation of a denser, more cohesive structure with improved interlayer adhesion. Conversely, the lower shear stress observed in Group 6 reflects the influence of increased layer height and extrusion width, which result in higher void content and weaker bonding between layers.

The shear properties, specifically shear strength and shear modulus, are depicted in Figure 5B,C, respectively. The results highlight the influence of layer height and line width on the mechanical performance of 3D-printed composite specimens. Group 1, fabricated with a layer height of 0.4 mm and a line width of 1.0 mm, exhibited the highest shear strength of 42.83 MPa. As the layer height and extrusion width increased, a progressive decline in shear strength was observed, with Groups 2, 3,

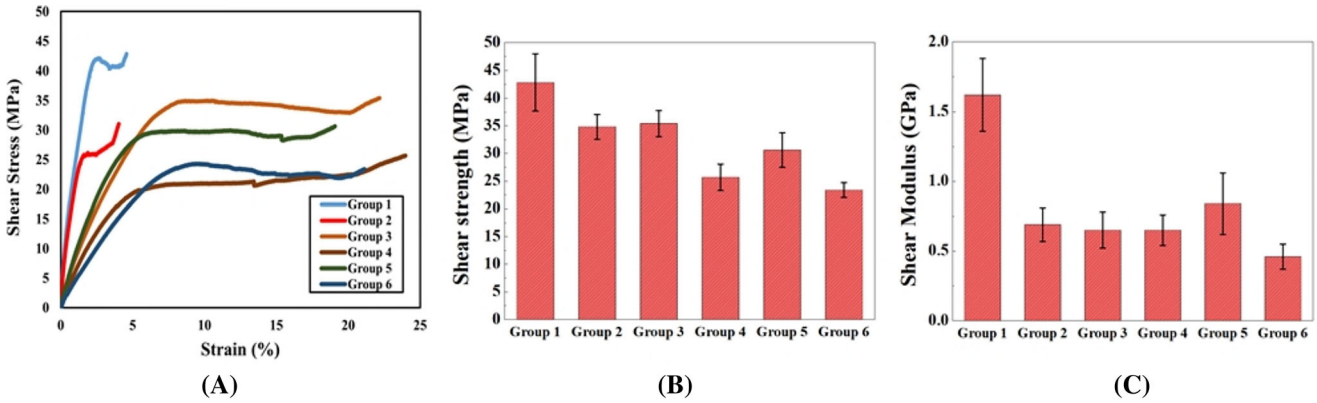

FIGURE 5 Shear properties of 3D-printed CCFRTCs using FFF: (A) Shear stress–strain curves from v-notched specimens; (B) average shear strength; (C) Shear modulus.

4, and 5 recording shear strengths of 34.83, 35.41, 25.67, and 30.61 MPa, respectively. Group 6, with the largest layer height and line width, demonstrated the lowest shear strength at 23.37 MPa.

Similarly, the shear modulus followed a comparable trend. Group 1 achieved the highest modulus of 1.62 GPa, while Group 6 exhibited the lowest modulus at 0.46 GPa. The results clearly indicate that increasing layer thickness and extrusion width adversely affect shear properties. This reduction can be attributed to the formation of higher void content and weaker interlayer adhesion, which diminish the composite's ability to resist shear forces. Shear strength is particularly sensitive to interlayer cohesion. A denser printed structure from smaller line width and layer height reduces interlayer slippage and enhances resistance to shear forces. Groups with higher void content (e.g., Group 6) exhibited early delamination and localized shear failure, leading to lower strength.

Notably, layer height was identified as the more critical parameter influencing the shear properties of the 3D-printed composite structures, consistent with prior findings for tensile and flexural properties.[22] The results emphasize the importance of optimizing layer height to enhance the structural density and interlayer bonding, thereby improving the shear performance of continuous carbon fiber-reinforced thermoplastic composites.

3.4 | Compressive properties

Figure 6A illustrates the compressive stress–strain curves for six distinct CCFRTC specimens fabricated with varying layer heights and line widths. These curves reveal the significant impact of printing parameters on the compressive behavior of the composite specimens. The observed trends align with those seen in tensile, flexural, and shear loading tests.

Group 1, with the smallest layer height and line width (0.4 and 1.0 mm, respectively), exhibited the highest compressive stress–strain curve, indicating superior compressive performance. This was followed by Groups 3, 2, 5, and 4, with Group 6 showing the lowest compressive stress levels. The superior performance of Group 1 can be attributed to its denser structure, resulting from reduced void content and improved interlayer adhesion due to optimized layer height and line width settings. Conversely, the lower performance of Group 6 highlights the detrimental effects of increased layer height and extrusion width, which lead to higher void content, reduced material density, and weaker interlayer bonding.

The compressive strength and modulus for the six CCFRTC groups are presented in Figure 6B,C, respectively. The results highlight the significant influence of layer height and line width on the compressive properties of the composite specimens. Group 1, fabricated with a layer height of 0.4 mm and line width of 1 mm, achieved the highest compressive strength and modulus, reaching 184.19 MPa and 4.48 GPa, respectively.

As the layer height and line width increased, the compressive strength and modulus progressively decreased. Groups 2, 3, 4, and 5 exhibited compressive strengths of 166.19, 177.40, 91.78, and 141.04 MPa, respectively. Group 6 demonstrated the lowest compressive strength and modulus, measuring 81.25 MPa and 3.47 GPa, respectively. The decline in mechanical properties with increasing layer height and line width is attributed to the increased presence of voids and reduced interlayer bonding, which weaken the composite structure and diminish its ability to resist compressive loads.

The compressive strength results showed significant variations with changes in layer height, emphasizing its critical impact on the mechanical performance of 3D-printed composites. For instance, when the layer height was reduced to 0.4 mm with a line width of 1.4 mm in

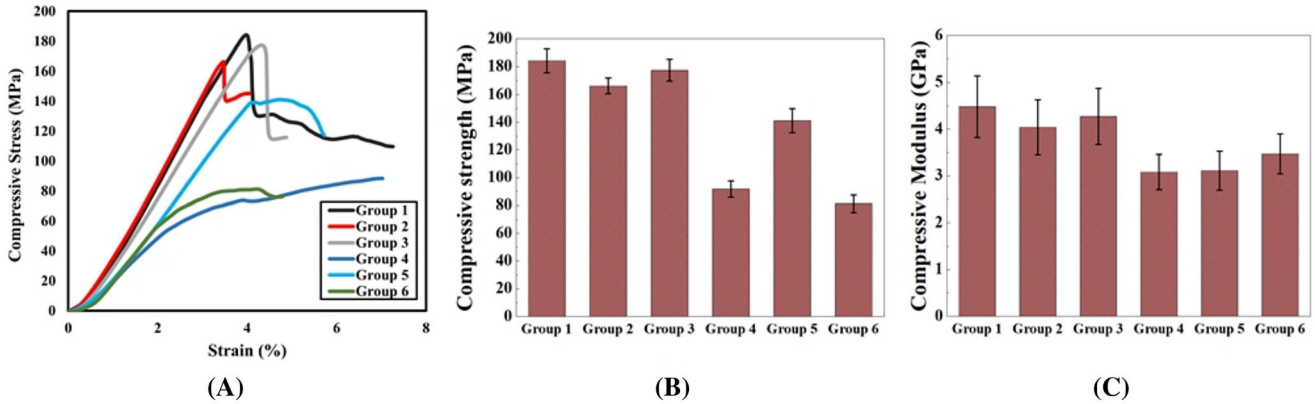

FIGURE 6 Compressive properties of 3D-printed CCFRTCs using FFF: (A) Compressive stress–strain curves; (B) average compressive strength; (C) Compressive modulus.

Group 5, the compressive strength increased by 53.7% compared to Group 4, highlighting the substantial influence of layer height on compressive strength. This effect was more pronounced in compressive loading compared to tensile, flexural, and shear strengths. The primary reason for this enhanced performance is the alignment of the compressive force with the direction of the printed fibers and composite layers. A lower layer height results in a tightly packed structure with improved layer arrangement, providing stronger interlayer adhesion and bonding. This structural compactness enables the composite to better withstand compressive loads by reducing voids and enhancing load distribution across the layers. Compression performance benefits from better structural packing and reduced void propagation paths. In Group 1, improved fiber alignment and close interfacial contact between layers prevented buckling and localized collapse under axial loads. In contrast, higher void content in Group 6 led to instability, crack initiation, and early failure. These findings underscore the importance of optimizing layer height to achieve higher compressive strength.

Overall, the mechanical performance trends are strongly influenced by geometrical compaction, fiber continuity, and void minimization, all of which are governed by the selected printing parameters. The results are supported by microstructural SEM analysis (Section 3.5), which shows clearer fiber-matrix bonding in better-performing groups. As a summary, Table 4 presents the mechanical properties of each composite group measured in this investigation.

3.5 | Fracture interface microstructural analysis

To comprehensively analyze the fracture interface behavior of the composite specimens, a representative sample from each group was selected based on the most significant failure mode observed in the tensile test results. The objective of this analysis was to evaluate the fracture performance, understand the deformation mechanisms during tensile loading, and investigate the adhesion behavior between the fiber and the polymer matrix. Following the mechanical testing, the fractured composite specimens were examined under SEM to capture high-resolution images of the ruptured regions, enabling a detailed assessment of the fiber-matrix interaction and failure characteristics.

The failure behavior of fiber-reinforced thermoplastic composites under mechanical loading is governed by several mechanisms, including fiber pullout, matrix cracking, delamination, interfacial debonding, and fiber breakage. The observed failure modes in this study were consistent across all mechanical tests but varied in severity depending on the printing parameters.

Figure 7 presents SEM images of the fractured regions from each composite group after tensile loading. The results indicate that all 3D-printed polymer composites exhibited a similar fracture mode, characterized by fiber-matrix separation, fiber pullout, and micro-cracking. Further, it illustrates the fractured zones, highlighting the detachment of carbon fibers from the matrix and the presence of void spaces formed during the tensile test. The separation of CCF from the polymer matrix is clearly visible, with distinct fiber and matrix regions observed, indicating the occurrence of fiber pullout (Figure 7B). The formation of micro-cracks is primarily attributed to fiber debonding and pullout from the matrix under tensile stress.

Despite the observed gaps and cracks, the SEM analysis also reveals instances where the matrix retained its hold on the carbon fibers, suggesting localized fiber-matrix adhesion and reinforcement integrity at various

TABLE 4 Summary of mechanical properties (mean ± SD) for each composite group.

Specimens	Mechanical properties							
	Tensile properties		Flexural properties		Shear properties		Compressive properties	
	Tensile strength (MPa)	Young's Modulus (GPa)	Flexural Strength (MPa)	Flexural Modulus (GPa)	Shear strength (MPa)	Shear Modulus (GPa)	Compressive strength (MPa)	Compressive Modulus (GPa)
Group 1	372.68 ± 11.84	41.63 ± 0.357	247.59 ± 15.32	29.13 ± 2.12	42.83 ± 5.16	1.62 ± 0.26	184.19 ± 8.60	4.48 ± 0.66
Group 2	315.82 ± 9.30	34.16 ± 0.48	210.48 ± 17.63	24.70 ± 2.18	34.83 ± 2.24	0.69 ± 0.12	166.19 ± 5.77	4.04 ± 0.59
Group 3	316.05 ± 14.80	39.43 ± 0.39	218.99 ± 19.71	23.94 ± 1.85	35.41 ± 2.34	0.65 ± 0.13	177.40 ± 7.73	4.27 ± 0.60
Group 4	247.28 ± 8.40	28.98 ± 0.42	180.23 ± 14.30	16.44 ± 1.33	25.67 ± 2.40	0.65 ± 0.11	91.78 ± 5.85	3.08 ± 0.38
Group 5	298.92 ± 9.39	32.02 ± 0.38	197.81 ± 11.05	20.15 ± 2.60	30.61 ± 3.13	0.84 ± 0.22	141.06 ± 8.63	3.11 ± 0.42
Group 6	231.04 ± 7.49	26.17 ± 0.48	170.70 ± 11.73	11.26 ± 1.12	23.37 ± 1.35	0.46 ± 0.09	81.25 ± 6.24	3.47 ± 0.43

points (Figure 7D). This indicates that, although some regions exhibited interfacial debonding, effective load transfer was achieved up to a critical stress threshold before failure occurred.

The occurrence of fiber pullout is a well-documented failure mechanism in fiber-reinforced polymer composites and is typically observed when the fiber-matrix interface bond strength is lower than the intrinsic tensile strength of the fibers.[46] The presence of fiber pullout zones suggests interfacial weakness, which may result from suboptimal fiber surface treatment, inadequate matrix infiltration during processing, or insufficient bonding interactions.

Additionally, the matrix material exhibited visible cracks and fissures, which likely originated at stress concentration points along the fiber-matrix interface. These cracks propagated through the matrix, indicative of brittle fracture behavior, where rapid crack growth occurred due to localized stress accumulation. The presence of fractured fibers within the matrix suggests that, in some instances, the fibers reached their ultimate tensile strength before interface failure occurred, reinforcing the effectiveness of load transfer within the composite structure. The primary failure mechanism of CCFRPCs was identified as fiber damage and fiber pullout, a characteristic weakness observed in 3D-printed CCF composite components.[14,47] The most significant defect contributing to failure in these specimens was fiber rip-out, which directly correlates with the degree of interfacial adhesion and fiber-matrix bonding strength.

Figure 7F highlights a region where carbon fibers remain embedded within the matrix, demonstrating effective adhesion in localized areas and indicating that load transfer between fibers and the matrix was successful up to a certain limit. However, the formation of voids and micro-fractures suggests the presence of processing defects or stress-induced debonding that occurred during tensile loading. These voids may be attributed to insufficient matrix infiltration, air entrapment during manufacturing, or localized stress concentrations at the fiber-matrix interface.

The fiber pullout phenomenon occurs when the interfacial bonding strength between the fiber and matrix is weaker than the tensile strength of the fiber itself. This can result from several factors, including inadequate fiber surface treatment, improper matrix infiltration, and limited interfacial bonding interactions.[48,49]

Under tensile loading, the dominant failure mechanisms observed were fiber pullout and fiber–matrix debonding, particularly in samples with higher layer heights and wider line widths (e.g., Group 6). SEM images revealed significant interfacial separation and void presence, indicating poor adhesion between the PLA

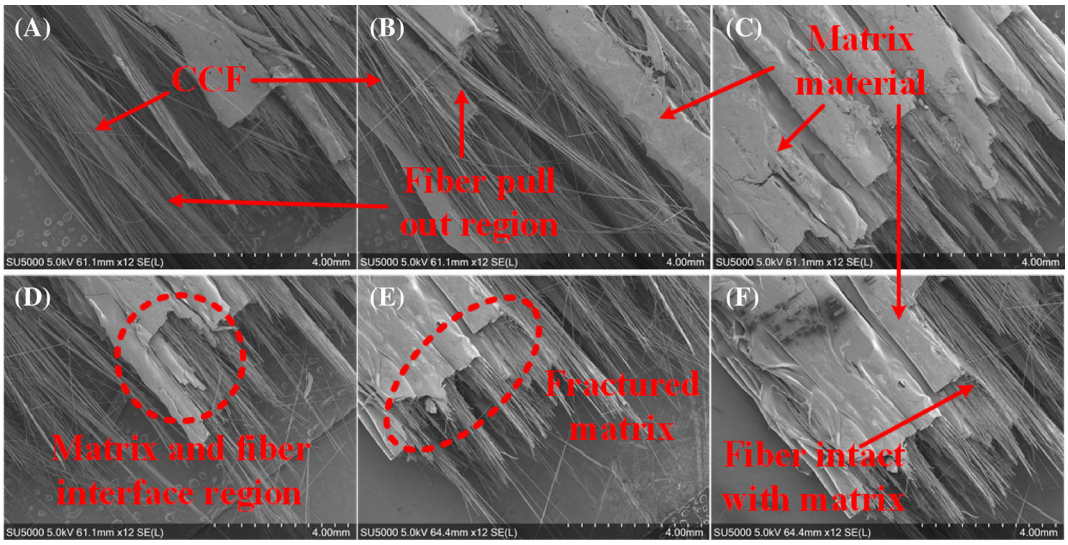

FIGURE 7 SEM micrographs of fractured composite specimens after the tensile test of (A) Group 1, (B) Group 2, (C) Group 3, (D) Group 4, (E) Group 5, (F) Group 6.

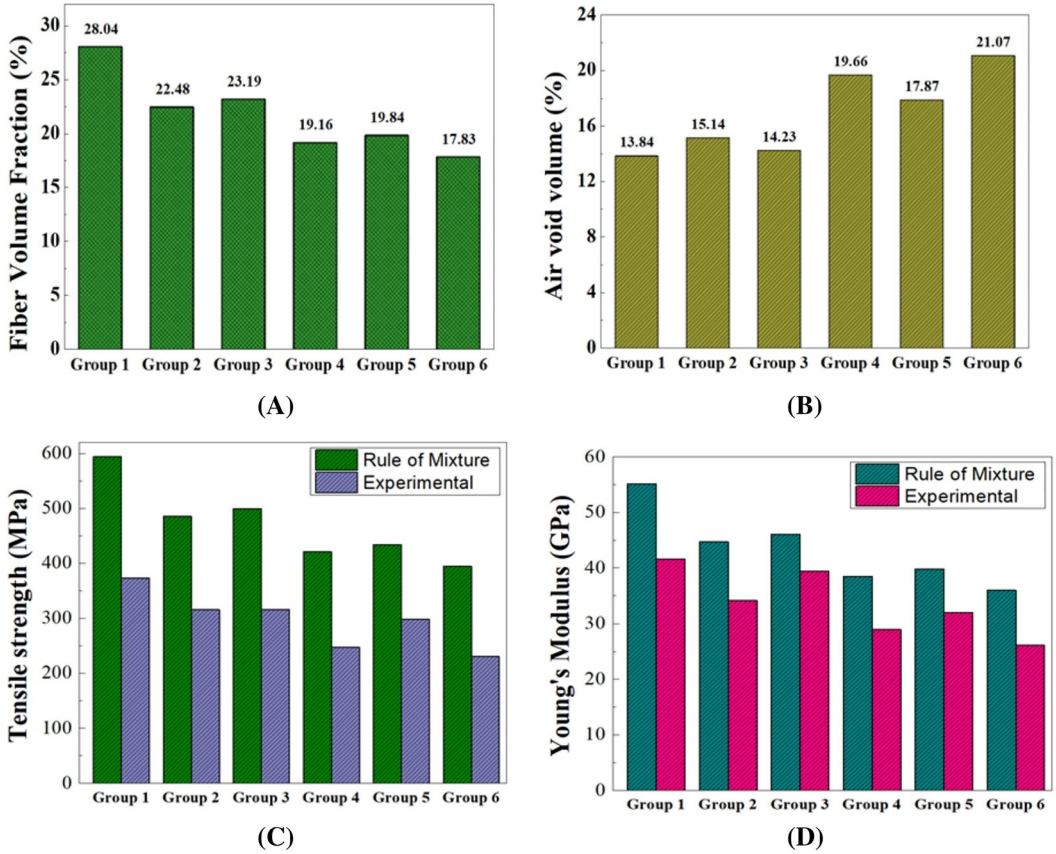

FIGURE 8 Composite characteristics across different parameter groups: (A) Estimated fiber volume fraction (V_f); (B) Air void content; (C) Experimental versus theoretical tensile strength using ROM; (D) Experimental versus predicted Young's modulus.

matrix and the carbon fiber. In contrast, Group 1 showed partial fiber breakage and less pullout, suggesting stronger interfacial bonding that allowed higher stress transfer to the fibers before failure. The presence of clean fiber surfaces in low-performing groups is further evidence of interfacial failure rather than cohesive fiber rupture.

During bending, failure typically initiated at the tensile side of the beam. Groups with better fiber alignment

and reduced voids exhibited progressive matrix cracking followed by fiber fracture, while others showed delamination between printed layers, a sign of weak interlayer adhesion. Compressive failures were governed by microbuckling and fiber kinking, especially in samples with higher porosity. The compact structure of Group 1 provided higher resistance to such instability. Shear loading, tested using notched specimens, revealed interlaminar shear failure and matrix yielding. In specimens with higher void content, crack initiation occurred at the notch roots, followed by propagation along weak interlayer regions. Fiber alignment perpendicular to the loading plane helped resist shear deformation in well-printed samples.

Higher layer heights and line widths contributed to greater void content and poorer interfacial contact, which directly translated into more brittle failure modes. Conversely, reduced voids and denser layer stacking in optimized groups improved energy dissipation, resulting in more ductile and progressive failure mechanisms. This clearly illustrates how microstructural features driven by process parameters influence macroscopic failure behavior.

3.6 | Volume fraction of the fiber

The CCF content within the composite specimens was estimated based on the tool path length, the number of lines, and the layers in terms of thickness and width. Reducing the layer height and line width in composite specimens with the same overall dimensions increases the number of lines and layers within the structure. This variation directly impacts the fiber content within the 3D-printed composite part. Figure 8A illustrates the estimated reinforcement content V_f of the CCF in the additively manufactured composite specimens. Group 1 demonstrated the highest V_f at 28.04%, followed by Group 3 (23.19%), Group 2 (22.48%), Group 5 (19.84%), Group 4 (19.16%), and Group 6 with the lowest V_f of 17.83%. The increase in layer count and line density due to reduced layer height and line width contributes to the higher fiber content in the structure, which in turn enhances the overall V_f. These V_f results provide a clear explanation for the mechanical properties observed in the specimens. Groups with higher V_f, such as Group 1, consistently achieved superior mechanical performance, exhibiting higher strength and modulus levels. Conversely, lower reinforcement content, as seen in Group 6, resulted in diminished mechanical properties. This correlation highlights the critical role of reinforcement content in determining the mechanical behavior of CCFRTC, emphasizing the importance of optimizing layer height and line width to achieve desired performance characteristics.

3.7 | Air void content in the manufactured composites

The void content of the 3D-printed polymer composite groups is presented as a bar graph in Figure 8B. The results show a clear relationship between printing parameters and the air void volume within the composite structures. Group 6 exhibited the highest void content at 21.07%, while Group 1 demonstrated the lowest void content at 13.84%. The void contents for Groups 2, 3, 4, and 5 were 15.14%, 14.23%, 19.66%, and 17.87%, respectively. The findings indicate that reducing the layer height and extrusion width significantly minimizes void content. These parameters contribute to the formation of more compact and dense structures by reducing the vacant spaces between layers and lines during the printing process.[22,27] This densification leads to improved interlayer adhesion and reduced porosity, enhancing the structural integrity of the composite specimens. These results underscore the importance of optimizing printing process parameters to control void volume, as lower void content is directly correlated with improved mechanical properties and performance.

3.8 | Rule of mixtures to predict elastic modulus and tensile strength

The rule of mixtures (ROM) has been implemented to predict the elastic modulus and tensile strength of additively manufactured CCFRTC with different layer height and line width. Varying both the parameters resulted in diverse tensile properties. Each group showed individual elastic modulus, since the composites were manufactured using same thermoplastic matrix and CF. Thus, according to the ROM, the predicted Young's modulus (E_c) and

TABLE 5 Predicted Young's modulus (E_c) and tensile strength (X_c) using ROM.

Composite's group	Predicted Young's modulus (E_c) (GPa)	Predicted Tensile strength (X_c) (MPa)
Group 1	55.14	594.33
Group 2	44.72	485.72
Group 3	46.05	499.59
Group 4	38.50	420.87
Group 5	39.78	434.15
Group 6	36.01	394.89

tensile strength (X_c) are calculated by the following expressions[50]:

$$E_c = V_f E_f + (1 - V_f) E_m \quad (2)$$

$$X_c = V_f X_f + (1 - V_f) X_m \quad (3)$$

where V_f is the volume fraction of the fiber; E_f and E_m are Young's moduli of the fiber and the matrix respectively; X_f and X_m are the tensile strength of the fiber and the matrix, respectively.

This approach is called the equal strength analysis model (ESA). This model is designed based on three primary assumptions: (a) linear elastic behavior till failure; (b) equal longitudinal strain in fiber, matrix, and composite; and (c) the load-carrying capacity of matrix after fiber failure is minimal.[51] Table 5 shows the numerical values of the Young's modulus and tensile strength of 3D printed composites predicted using ROM. A comparison of the tensile strength and Young's modulus has been made between the experimental and theoretical predictions and are plotted together and shown in Figure 8C,D, respectively. Table 5 presents the predicted Young's modulus (E_c) and tensile strength (X_c) values using ROM.

The results show the consistent trend of the results obtained experimentally. As observed from Figure 8C,D, the experimental results of tensile strength and Young's modulus and are always lower than the ROM prediction. However, the printing parameters (layer height and line width) have shown the even results that were achieved experimentally and evident that it has influence on the tensile properties. Although, for the same thermoplastic matrix and reinforcement material, both the experimental and the theoretical prediction results show that an increase in fiber content can significantly improve the tensile strength and elastic modulus of the composite specimen. Moreover, the prediction of Young's modulus by ROM is close to the experimentally achieved modulus, whereas the prediction of tensile strength shows a large deviation from the experimental results. The strength can be affected by various factors, such as the non-uniform arrangement of continuous fibers, insufficient interlaminar bonding between the fibers and matrix that cause voids and microcracks intrinsic in the 3D printed composite structure that lead to premature failure.[52]

4 | CONCLUSIONS

The experimental study presented the manufacturing of CCFRTC using co-extrusion with towpreg utilizing material extrusion technology with a modified extrusion head with dual input and a single extrusion nozzle. The study demonstrated the significant influence of the printing process parameters on the mechanical properties, volume fraction, and air void content of 3D printed composites. Six groups of composite specimens were printed using different layer heights and extrusion line widths. These parameters were selected due to their notable impact on the printed structures' mechanical properties. The results revealed that the composite specimen printed with a layer height of 0.4 mm and a line width of 1 mm reached the maximum tensile, flexural, shear, and compressive strength of 372.68, 247.59, 42.83, and 184.19 MPa, respectively. Increasing both parameters tends to decrease the mechanical properties. In comparison of both printing parameters, the layer height of the printed structure has more impact on the mechanical performance. The same group also showed the highest V_f content of 28.04% with the minimum air voids of 13.84%. The results of the additively manufactured CCFRTC using co-extrusion with towpreg evidenced that lower layer height and line width formed a more compact structure with better adhesion bonding, higher fiber content, and fewer air voids, thus leading to better performance when subject to mechanical loadings in tension, bending, shear, and compression. It was also shown that a linear rule of mixing is capable of predicting the observed trends but significantly underpredicts the strength values. This study contributes to the growing body of work on fiber-reinforced additive manufacturing by showing how process tuning can significantly affect structural integrity. While only two parameters were studied, the insights gained lay the groundwork for broader optimization studies involving print speed, nozzle temperature, fiber tension, and multi-directional reinforcement. Future work will focus on expanding the parametric space, incorporating statistical design of experiments (DOE), and exploring high-performance thermoplastics (e.g., PEEK, PEKK) for demanding applications in aerospace and automotive sectors.

AUTHOR CONTRIBUTIONS

Nabeel Maqsood: Conceptualization, data curation, formal analysis, investigation, methodology, visualization, writing – original draft. **Genrik Mordas:** Formal analysis, investigation, resources, validation, visualization, writing – review & editing. **Marius Rimašauskas:** Data curation, formal analysis, investigation, supervision, validation, writing – review & editing. **Kateřina Skotnicová:** Formal analysis, validation, resources, project administration, writing – review & editing, funding acquisition. **Jawad Ullah:** Data curation, formal analysis, investigation, methodology, validation, Writing – review & editing. **Joamin Gonzalez-Gutierrez:** Investigation, methodology, validation, visualization, writing – review & editing.

ACKNOWLEDGMENT

Open access publishing facilitated by Vysoka skola banska-Technicka univerzita Ostrava, as part of the Wiley - CzechELib agreement.

FUNDING INFORMATION

This article has been produced with the financial support of the European Union under the REFRESH – Research Excellence For REgion Sustainability and High-tech Industries project number CZ.10.03.01/00/22_003/0000048 via the Operational Programme Just Transition.

CONFLICT OF INTEREST STATEMENT

The authors declare that they have no known competing interests or personal relationships that could have appeared to influence the work reported in this paper.

DATA AVAILABILITY STATEMENT

The datasets used and/or analyzed during the current study are available from the corresponding author on reasonable request.

ORCID

Nabeel Maqsood https://orcid.org/0000-0003-4875-471X
Marius Rimašauskas https://orcid.org/0000-0002-5064-7107
Kateřina Skotnicová https://orcid.org/0000-0002-7887-140X
Jawad Ullah https://orcid.org/0000-0003-4441-1277
Joamin Gonzalez-Gutierrez https://orcid.org/0000-0003-4737-9823

REFERENCES

1. Dong W, Bao C, Lu W, et al. Fabrication of a continuous carbon fiber-reinforced phenolic resin composites via in situ-curing 3D printing technology. *Compos Commun*. 2023;38:101497. doi:10.1016/j.coco.2023.101497
2. Maqsood N, Mahato S, Rimašauskas M, Muna II. Experimental analysis, analytical approach and numerical simulation to estimate the elastic modulus of 3D printed CCFRPC under mechanical loadings. *J Braz Soc Mech Sci Eng*. 2023;45:1-15. doi:10.1007/s40430-023-04408-2
3. Ivanova O, Williams C, Campbell T. Additive manufacturing (AM) and nanotechnology: promises and challenges. *Rapid Prototyp J*. 2013;19:353-364. doi:10.1108/RPJ-12-2011-0127
4. Karaş B, Smith PJ, Fairclough JPA, Mumtaz K. Additive manufacturing of high density carbon fibre reinforced polymer composites. *Addit Manuf*. 2022;58:103044. doi:10.1016/j.addma.2022.103044
5. Abd El Aal MI, Awd Allah MM, Abd Alaziz SA, Abd El-baky MA. Biodegradable 3D printed polylactic acid structures for different engineering applications: effect of infill pattern and density. *J Polym Res*. 2024;31:4. doi:10.1007/s10965-023-03852-x
6. Criado-Gonzalez M, Dominguez-Alfaro A, Lopez-Larrea N, Alegret N, Mecerreyes D. Additive manufacturing of conducting polymers: recent advances, challenges, and opportunities. *ACS Appl Polym Mater*. 2021;3:2865-2883. doi:10.1021/acsapm.1c00252
7. Tian X, Todoroki A, Liu T, et al. 3D printing of continuous fiber reinforced polymer composites: development, application, and prospective. *Chin J Mech Eng Addit Manuf Front*. 2022;1:100016. doi:10.1016/j.cjmeam.2022.100016
8. Maqsood N, Zaheer MD. Fabrication of cellular composite structures with continuous fiber reinforcement and different infill patterns using fused filament fabrication. *Addit Manuf Front*. 2024;3:200156. doi:10.1016/j.amf.2024.200156
9. Karimi A, Rahmatabadi D, Baghani M. Various FDM mechanisms used in the fabrication of continuous-fiber reinforced composites: a review. *Polymers (Basel)*. 2024;16:831. doi:10.3390/polym16060831
10. Li J, Durandet Y, Huang X, Sun G, Ruan D. Additively manufactured fiber-reinforced composites: a review of mechanical behavior and opportunities. *J Mater Sci Technol*. 2022;119:219-244. doi:10.1016/j.jmst.2021.11.063
11. Nuge T, Fazeli M, Baniasadi H. Elucidating the enduring transformations in cellulose-based carbon nanofibers through prolonged isothermal treatment. *Int J Biol Macromol*. 2024;275:133480. doi:10.1016/j.ijbiomac.2024.133480
12. Safari F, Kami A, Abedini V. 3D printing of continuous fiber reinforced composites: a review of the processing, pre- and post-processing effects on mechanical properties. *Polym Polym Compos*. 2022;30:096739112210987. doi:10.1177/09673911221098734
13. Feng J, Yao L, Lyu Z, Wu Z, Zhang G, Zhao H. Mechanical properties and damage failure of 3D-printed continuous carbon fiber-reinforced composite honeycomb sandwich structures with fiber-interleaved core. *Polym Compos*. 2023;44:1980-1992. doi:10.1002/pc.27221
14. Maqsood N, Rimašauskas M. Research of continuous carbon fiber content in porous composite structures produced by using additive manufacturing technology. *Macromol Symp*. 2022;404:2100429. doi:10.1002/masy.202100429
15. Fazeli M, Islam S, Baniasadi H, et al. Exploring the potential of regenerated ioncell fiber composites: a sustainable alternative for high-strength applications. *Green Chem*. 2024;26:6822-6835. doi:10.1039/D3GC03637E
16. Wu Y, Wang K, Neto V, Peng Y, Valente R, Ahzi S. Interfacial behaviors of continuous carbon fiber reinforced polymers manufactured by fused filament fabrication: a review and prospect. *Int J Mater Form*. 2022;18:1-18. doi:10.1007/s12289-022-01667-7
17. Xin Z, Ma Y, Chen Y, Wang B, Xiao H, Duan Y. Fusion-bonding performance of short and continuous carbon fiber synergistic reinforced composites using fused filament fabrication. *Compos B: Eng*. 2023;248:110370. doi:10.1016/j.compositesb.2022.110370
18. Green JT, Rybak IA, Slager JJ, et al. Local composition control using an active-mixing hotend in fused filament fabrication. *Addit Manuf Lett*. 2023;7:100177. doi:10.1016/j.addlet.2023.100177
19. Matschinski A. Integration of Continuous Fibers in Additive Manufacturing Processes, Virtual Symposium on AFP and AM, Technical University of Munich and Australian National University. 2020.
20. Wang F, Wang G, Wang H, Fu R, Lei Y, He J. 3D printing Technology for Short-continuous Carbon Fiber Synchronous

Reinforced Thermoplastic Composites: a comparison between Towpreg extrusion and in situ impregnation processes. *Chin J Mech Eng Add Manuf Front*. 2023;2:100092. doi:10.1016/j.cjmeam.2023.100092

21. Maqsood N, Rimašauskas M. Tensile and flexural response of 3D printed solid and porous CCFRPC structures and fracture interface study using image processing technique. *J Mater Res Technol*. 2021;14:731-742. doi:10.1016/j.jmrt.2021.06.095
22. Rimašauskas M, Jasiūnienė E, Kuncius T, Rimašauskienė R, Cicėnas V. Investigation of influence of printing parameters on the quality of 3D printed composite structures. *Compos Struct*. 2022;281:115061. doi:10.1016/j.compstruct.2021.115061
23. Heidari-Rarani M, Rafiee-Afarani M, Zahedi AM. Mechanical characterization of FDM 3D printing of continuous carbon fiber reinforced PLA composites. *Compos B: Eng*. 2019;175:107147. doi:10.1016/j.compositesb.2019.107147
24. Fidan I, Imeri A, Gupta A, et al. The trends and challenges of fiber reinforced additive manufacturing. *Int J Adv Manuf Technol*. 2019;102:1801-1818. doi:10.1007/s00170-018-03269-7
25. Adil S, Lazoglu I. A review on additive manufacturing of carbon fiber-reinforced polymers: current methods, materials, mechanical properties, applications and challenges. *J Appl Polym Sci*. 2023;140:1-28. doi:10.1002/app.53476
26. Awd Allah MM, Abd El-Halim MF, Almuflih AS, Mahmoud SF, Saleh DI, Abd El-baky MA. Innovative, high-performance, and cost-effective hybrid composite materials for crashworthiness applications. *Polym Compos*. 2025;46:11832-11853. doi:10.1002/pc.29714
27. Maqsood N, Rimašauskas M. Influence of printing process parameters and controlled cooling effect on the quality and mechanical properties of additively manufactured CCFRPC. *Compos Commun*. 2022;35:101338. doi:10.1016/j.coco.2022.101338
28. Peng X, Zhang M, Guo Z, Sang L, Hou W. Investigation of processing parameters on tensile performance for FDM-printed carbon fiber reinforced polyamide 6 composites. *Compos Commun*. 2020;22:100478. doi:10.1016/j.coco.2020.100478
29. Ramesh M, Rajeshkumar L, Balaji D. Influence of process parameters on the properties of additively manufactured fiber-reinforced polymer composite materials: a review. *J Mater Eng Perform*. 2021;30:4792-4807. doi:10.1007/s11665-021-05832-y
30. Awd Allah MM, Abd El-Halim MF, Abbas MA, Almuflih AS, Saleh DI, Abd El-baky MA. Discovering the impact of printing parameters on the crashworthiness performance of 3D-printed cellular structures. *Fibers Polym*. 2025;26:297-315. doi:10.1007/s12221-024-00799-8
31. Awd Allah MM, Abd El-Halim MF, Sebaey TA, Mahmoud SF, Saleh DI, Abd El-baky MA. Multi-criteria decision-making for optimizing crashworthiness of 3D-printed PETG-CF lightweight structures: influence of printing parameters. *Polym Compos*. 2025;46(S1):S940-S963. doi:10.1002/pc.29826
32. Dou H, Cheng Y, Ye W, et al. Effect of process parameters on tensile mechanical properties of 3D printing continuous carbon fiber-reinforced PLA composites. *Materials (Basel)*. 2020;13:3850. doi:10.3390/ma13173850
33. Moradi M, Moghadam MK, Shamsborhan M, Bodaghi M. The synergic effects of fdm 3D printing parameters on mechanical behaviors of bronze poly lactic acid composites. *J Compos Sci*. 2020;4:1-16. doi:10.3390/jcs4010017
34. Pentek A, Nyitrai M, Schiffer A, et al. The effect of printing parameters on electrical conductivity and mechanical properties of PLA and ABS based carbon composites in additive manufacturing of upper limb prosthetics. *Crystals*. 2020;10:1-12. doi:10.3390/cryst10050398
35. Christiyan KGJ, Chandrasekhar U, Venkateswarlu K. A study on the influence of process parameters on the mechanical properties of 3D printed ABS composite. *IOP Conf Ser Mater Sci Eng*. 2016;114:012109. doi:10.1088/1757-899X/114/1/012109
36. Nabipour M, Akhoundi B. An experimental study of FDM parameters effects on tensile strength, density, and production time of ABS/Cu composites. *J Elastomers Plast*. 2021;53:146-164. doi:10.1177/0095244320916838
37. Chen K, Yu L, Cui Y, Jia M, Pan K. Optimization of printing parameters of 3D-printed continuous glass fiber reinforced polylactic acid composites. *Thin-Walled Struct*. 2021;164:107717. doi:10.1016/j.tws.2021.107717
38. Zhang H, Wang J, Liu Y, Zhang X, Zhao Z. Effect of processing parameters on the printing quality of 3D printed composite cement-based materials. *Mater Lett*. 2022;308:131271. doi:10.1016/j.matlet.2021.131271
39. Rimašauskas M, Kuncius T, Rimašauskienė R. Processing of carbon fiber for 3D printed continuous composite structures. *Mater Manuf Process*. 2019;34:1528-1536. doi:10.1080/10426914.2019.1655152
40. Li N, Li Y, Liu S. Rapid prototyping of continuous carbon fiber reinforced polylactic acid composites by 3D printing. *J Mater Process Technol*. 2016;238:218-225. doi:10.1016/j.jmatprotec.2016.07.025
41. Tian X, Liu T, Yang C, Wang Q, Li D. Interface and performance of 3D printed continuous carbon fiber reinforced PLA composites. *Compos Part A: Appl Sci Manuf*. 2016;88:198-205. doi:10.1016/j.compositesa.2016.05.032
42. Diouf-Lewis A, Farahani RD, Iervolino F, et al. Design and characterization of carbon fiber-reinforced PEEK/PEI blends for fused filament fabrication additive manufacturing. *Mater Today Commun*. 2022;31:103445. doi:10.1016/j.mtcomm.2022.103445
43. ASTM D3171-22. *Standard Test Methods for Constituent Content of Composite Materials*. ASTM Int. 08; 2000:1-7. doi:10.1520/C1709-18
44. Muna II, Mieloszyk M, Rimasauskiene R, Maqsood N, Rimasauskas M. Thermal effects on mechanical strength of additive manufactured CFRP composites at stable and cyclic temperature. *Polymers (Basel)*. 2022;14:4680. doi:10.3390/polym14214680
45. Jiang X, Shan Z, Zang Y, Liu F, Wu X, Zou A. Effect of process parameters on tensile properties of 3D printed continuous aramid fiber reinforced nylon 12 composites. *J Thermoplast Compos Mater*. 2023;0:1-19. doi:10.1177/08927057231223925
46. Maqsood N, Rimašauskas M. Fracture Interface observation after the mechanical test of additively manufactured CCFRTC fabricated under the controlled air flow cooling effect. In: Bindhu V, Tavares JMRS, Chen JIZ, eds. *Proceedings of Fifth International Conference on Inventive Material Science Applications*, Advances in Sustainability Science and Technology. Springer; 2023:87-95. doi:10.1007/978-981-19-4304-1_8

47. Hao W, Liu Y, Zhou H, Chen H, Fang D. Preparation and characterization of 3D printed continuous carbon fiber reinforced thermosetting composites. *Polym Test*. 2018;65:29-34. doi:10.1016/j.polymertesting.2017.11.004
48. Maqsood N, Rimašauskas M, Ghobakhloo M, Mordas G, Skotnicová K. Additive manufacturing of continuous carbon fiber reinforced polymer composites using materials extrusion process. Mechanical properties, process parameters, fracture analysis, challenges, and future prospect. A review. *Adv Compos Hybrid Mater*. 2024;7:202. doi:10.1007/s42114-024-01035-w
49. Garoz Gómez D, Pascual-González C, García-Moreno Caraballo J, Fernández-Blázquez JP. Methodology to design and optimise dispersed continuous carbon fibre composites parts by fused filament fabrication. *Compos Part A: Appl Sci Manuf*. 2023;165:107315. doi:10.1016/j.compositesa.2022.107315
50. Zhang H, Sun W. Mechanical properties and failure behavior of 3D printed thermoplastic composites using continuous basalt fiber under high-volume fraction. *Def Technol*. 2023;27:237-250. doi:10.1016/j.dt.2022.07.010
51. Hetrick DR, Sanei SHR, Bakis CE, Ashour O. Evaluating the effect of variable fiber content on mechanical properties of additively manufactured continuous carbon fiber composites. *J Reinf Plast Compos*. 2021;40:365-377. doi:10.1177/0731684420963217
52. He Q, Wang H, Fu K, Ye L. 3D printed continuous CF/PA6 composites: effect of microscopic voids on mechanical performance. *Compos Sci Technol*. 2020;191:108077. doi:10.1016/j.compscitech.2020.108077

How to cite this article: Maqsood N, Mordas G, Rimašauskas M, Skotnicová K, Ullah J, Gonzalez-Gutierrez J. Investigation and assessment of mechanical properties of co-extrusion with towpreg continuous carbon fiber reinforced thermoplastic composites manufactured using material extrusion. *Polym Compos*. 2025;46(Suppl. 3):S867-S883. doi:10.1002/pc.30004